Journal of Neonatal Surgery
ISSN(Online): 2226-0439
Vol. 14, Issue 15s (2025)
https://www.jneonatalsurg.com

OPEN ACCESS

A Hybrid Approach for Alzheimer's Disease Diagnosis: Integrating NCA-Based Feature Selection with SVM, KNN, and ESO-Optimized Neural Networks

Ruchi Agarwal[1], Dr. Asha Ambhaikar[2]

[1]PhD Scholar, MATS University
Email ID: ragrawal3291@gmail.com
[2]Professor, Department of CSE, MATS University.
Email ID: drasha@matsuniversity.ac.in

Cite this paper as: Ruchi Agarwal, Dr. Asha Ambhaikar, (2025) A Hybrid Approach for Alzheimer's Disease Diagnosis: Integrating NCA-Based Feature Selection with SVM, KNN, and ESO-Optimized Neural Networks. *Journal of Neonatal Surgery*, 14 (15s), 482-508.

ABSTRACT

Alzheimer's disease (AD) is a progressive neurodegenerative disorder that poses significant challenges for early detection and accurate classification, crucial for effective intervention and management. In the realm of medical imaging and diagnostic classification, various machine learning techniques have been employed to enhance the precision of AD detection. This paper presents a novel framework for the detection and staging of AD using MRI brain images. The methodology begins with the acquisition of T1-weighted MRI scans from the OASIS database, followed by contrast enhancement through Contrast Limited Adaptive Histogram Equalization (CLAHE). The enhanced images are analyzed using a multi-faceted approach involving several feature extraction techniques. Discrete Wavelet Transform (DWT) combined with Local Binary Patterns (LBP) captures detailed texture features across multiple scales. Additionally, Histogram of Oriented Gradients (HOG) is utilized for structural feature extraction, and Speeded Up Robust Features (SURF) combined with Bag of Words (BoW) is employed for key point detection and representation. These features are integrated into a combined feature vector, which is then refined using Neighborhood Component Analysis (NCA) for optimal feature selection. Classification is performed using Support Vector Machine (SVM), K-Nearest Neighbors (KNN), and an Enhanced Snake Optimization (ESO)-optimized Neural Network. Performance evaluation metrics including accuracy, sensitivity, and specificity are used to validate the effectiveness of the proposed framework in AD detection and staging. The results indicate that the ESO-NN model, achieves the highest accuracy of 98.07% among the evaluated classifiers. This superior performance underscores the potential of ESO-NN in improving diagnostic accuracy and reliability, marking a significant advancement in the field of AD detection and classification.

Keywords: *Alzheimer's Disease, Bag of Words, CLAHE, Enhanced Snake Optimization, K-Nearest Neighbors, Local Binary Patterns, Neural Network, Support Vector Machine, SURF.*

1. INTRODUCTION

Alzheimer's disease (AD) is a growing global concern, particularly with an aging population. As the most prevalent form of dementia, AD causes a progressive decline in cognitive abilities, severely affecting memory, thinking, and behavior. The socio-economic impact of AD is profound, with millions affected worldwide, and this number is expected to increase significantly in the coming years. One of the major challenges in managing AD is the difficulty in early diagnosis and accurate staging, as effective treatment largely depends on timely intervention. By the time clinical symptoms are evident, considerable and often irreversible brain damage has usually occurred, underscoring the need for advanced diagnostic tools that can identify and stage AD in its earliest and most treatable phases.

Traditional diagnostic methods, such as cognitive tests and neuroimaging, while valuable, often lack the sensitivity needed to detect the subtle brain changes that characterize the early stages of AD. For instance, although Magnetic Resonance Imaging (MRI) provides detailed anatomical images of the brain, interpreting these images to identify minute structural changes indicative of early AD requires advanced analytical techniques. Despite rapid advances in neuroimaging, a gap remains in effectively integrating these innovations into clinical practice [1].

The complexity of AD further complicates diagnosis. AD does not manifest uniformly across individuals, and its progression involves a range of pathological changes, including amyloid plaques, neurofibrillary tangles, and neuronal loss. These changes typically begin in brain regions such as the hippocampus, which is crucial for memory formation, and gradually

spread, leading to widespread brain atrophy. However, the relationship between these pathological changes and the clinical symptoms of AD is intricate, making it challenging to establish clear diagnostic markers [1].

Recent advances in machine learning and artificial intelligence hold great promise for improving the diagnostic process for AD. Machine learning algorithms, especially those applied to image processing, have shown the ability to detect patterns in MRI images that are otherwise imperceptible to the human eye. These patterns may reflect changes in brain volume, texture, and structural integrity, all of which are indicative of AD's presence and progression. For instance, early signs of AD, such as changes in the hippocampus and surrounding brain regions, can be detected and analyzed using these advanced techniques. The gradual transition from normal aging to mild cognitive impairment (MCI) and eventually to Alzheimer's often blurs the lines between these stages, necessitating a more sophisticated classification approach that can distinguish these subtle differences [2].

Multi-feature analysis has emerged as a particularly promising approach in AD detection. By combining features that capture various aspects of the brain's structure and function—such as texture, shape, and volumetric changes—a more comprehensive representation of the disease can be constructed. For example, texture analysis can reveal microstructural changes in the brain, while volumetric analysis measures atrophy in key regions. However, the challenge lies in effectively integrating these diverse features and ensuring that the resulting model is both accurate and generalizable across different populations [3].

The selection of features is critical to the effectiveness of such diagnostic frameworks. Given the high dimensionality of the data, traditional feature selection methods may struggle to capture the most relevant features. This is where Neighborhood Component Analysis (NCA) becomes invaluable. NCA is a powerful feature selection technique that identifies the most informative features for classification by optimizing the distance between data points in the transformed feature space. This method enhances the classifier’s ability to distinguish between subtle patterns, significantly improving the overall diagnostic accuracy.

The significance of early and accurate staging of Alzheimer's disease cannot be overstated. Identifying individuals in the MCI stage, particularly those at high risk of progressing to AD, provides a crucial window for intervention. Current treatments for AD are most effective when administered early, before significant neurodegeneration has occurred. Thus, a framework that not only detects Alzheimer's but also stages the disease with precision can significantly impact patient outcomes by guiding treatment decisions.

This research aims to bridge the gap between early pathological brain changes and clinical diagnosis by developing a robust, multi-feature-based diagnostic tool that integrates advanced image processing techniques with optimized classifiers. By incorporating NCA for feature selection, the proposed framework ensures that the most relevant features are retained, significantly enhancing the model’s classification performance. The following sections will delve into the theoretical foundations of the proposed approach, review current research in the field, and present the methodologies used in developing this diagnostic framework.

This paper presents a significant advancement in AD detection and staging by introducing a novel and comprehensive hybrid framework. The major contributions of this research are as follows:

- **Contrast Enhancement via CLAHE:** The study begins by applying Contrast Limited Adaptive Histogram Equalization (CLAHE) to enhance the contrast in MRI images. CLAHE effectively amplifies subtle details in neuroimaging, thereby improving the visibility of critical features that may indicate early stages of AD. By adjusting the image contrast, CLAHE plays a crucial role in preparing the data for subsequent feature extraction processes, ensuring that the most important information is highlighted.
- **DWT-LBP for Advanced Texture Analysis:** The integration of Discrete Wavelet Transform (DWT) with Local Binary Patterns (LBP) provides a powerful method for texture feature extraction. DWT enables multi-resolution analysis, capturing both fine and coarse details, while LBP encodes local texture patterns. This combination is particularly effective in identifying the textural changes associated with Alzheimer's disease progression, offering a detailed representation of the brain's microstructural alterations.
- **HOG and SURF for Structural and Key Point Feature Extraction:** The methodology further incorporates Histogram of Oriented Gradients (HOG) and Speeded-Up Robust Features (SURF) for capturing structural and key point features. HOG contributes to detecting shape-related features by analyzing gradient orientations, while SURF efficiently identifies and describes key points in the neuroimaging data. This dual approach enhances the ability to detect both global structural changes and localized key points, essential for distinguishing between different AD stages.
- **Comprehensive Multi-Feature Integration:** The diverse features extracted through DWT-LBP, HOG, and SURF are integrated into a cohesive multi-feature set. This integration process combines various aspects of the data, including texture, structure, and key points, to form a comprehensive feature set. The synergy between these features provides a robust foundation for the classification process, ensuring that the model can accurately capture the

complex patterns associated with Alzheimer's disease.

- **Advanced Feature Selection with Neighborhood Component Analysis (NCA):** A key innovation in this research is the application of Neighborhood Component Analysis (NCA) for feature selection. NCA optimizes the feature space by selecting the most relevant features that contribute to accurate classification. By minimizing intra-class distances and maximizing inter-class distances in the feature space, NCA enhances the model's ability to distinguish between different stages of Alzheimer's disease. This step is crucial in handling the high-dimensional data derived from multi-feature integration, ensuring that the most informative features are retained for classification.
- **Optimized Classification through SVM, KNN, and ESO-Optimized Neural Network:** The classification framework utilizes a combination of Support Vector Machine (SVM), k-Nearest Neighbors (KNN), and an Enhanced Snake Optimization (ESO)-Optimized Neural Network. SVM is selected for its proficiency in handling high-dimensional data and finding the optimal decision boundaries, while KNN is employed for its simplicity and effectiveness in instance-based learning. The ESO-Optimized Neural Network represents a significant innovation in this work, where the Enhanced Snake Optimization algorithm is utilized to fine-tune the neural network's parameters. This optimization process enhances the neural network's ability to model intricate patterns within the data, leading to superior performance in AD classification.
- **Dual-Level Classification: Global and Local Staging:** The proposed framework excels in both global and local classification tasks. At a global level, the system is capable of distinguishing between normal cognitive function, mild cognitive impairment (MCI), and Alzheimer's disease. On a local level, the framework further refines the classification of MCI into distinct sub-categories: Very Mild Dementia (VMD), Mild Dementia (MD), and Moderate Dementia (MoD). This nuanced classification is essential for understanding the intricate progression of Alzheimer's disease and enabling timely interventions.

This paper contributes significantly to the field of Alzheimer's disease detection by proposing an innovative hybrid approach that integrates advanced image enhancement techniques with optimized classification algorithms, including feature selection through NCA. The framework not only improves diagnostic accuracy but also enhances the understanding of disease progression, paving the way for future research and clinical applications. The paper begins with a comprehensive literature review in Section 2, examining relevant studies in the field. Section 3 details the materials and methods employed in the research, followed by Section 4, which provides an in-depth explanation of the proposed methodologies. Section 5 presents the results obtained from MATLAB-based simulations, along with a detailed analysis. The paper concludes in Section 6, summarizing the findings and discussing their implications for future work.

2. LITERATURE REVIEW

In recent years, there has been a surge in research focused on the early detection and prediction of Alzheimer's disease (AD) [4]. The advancements in machine learning (ML) and deep learning (DL) techniques have significantly contributed to these efforts. For instance, the study presented in [5] developed a DL-based approach to differentiate between brains affected by Alzheimer's and those of healthy individuals. Their method utilized convolutional neural networks (CNNs), a key architecture in deep learning, to create a model for prediction and classification. The approach they proposed for detecting AD, mild cognitive impairment (MCI), and its early stages involved using a stacked autoencoder, a softmax regression layer, and a relatively small annotated dataset, which reduced the need for extensive prior experience. Nevertheless, this method has notable limitations, particularly in its reliance on a large amount of labeled data to achieve optimal results. The effectiveness of this approach was evaluated using neuroimaging data from 311 participants enrolled in the AD Neuroimaging Initiative (ADNI) study. This cohort included 65 individuals diagnosed with Alzheimer's disease, 67 with mild cognitive impairment (MCI) progressing toward AD, 102 with stable non-converting MCI (ncMCI), and 77 healthy control (NC) participants. When integrating both magnetic resonance imaging (MRI) and Positron Emission Tomography (PET) scans, the method achieved a binary classification accuracy of 88.58%. In contrast, the accuracy for a four-class classification task was lower, at 47.42%. In a related study by [6], a hybrid multi-class deep learning framework was proposed for the early detection of AD. This framework utilized an advanced version of the k-Sparse autoencoder (KSA) for classifying brain regions showing passive degeneration. The study involved 150 MRI scans along with cerebrospinal fluid (CSF) and PET images from the ADNI dataset. The enhanced KSA demonstrated improved accuracy compared to both the traditional zero-masking approach and the original KSA. Nonetheless, the effectiveness of this method is heavily influenced by the quality of the enhancement techniques employed.

In their quest to advance Alzheimer's disease diagnosis, the researchers in [7] proposed a 3D CNN framework that utilizes both MRI and PET imaging modalities. To enhance its performance, they incorporated an FSBi-LSTM component, which combines bidirectional long short-term memory with spatial information extracted from detailed feature maps. The framework was extensively tested using the ADNI dataset. It achieved diagnostic accuracies of 94.82% for differentiating AD from normal controls (NC), 86.36% for distinguishing progressive MCI (pMCI) from NC, and 65.35% for separating stable MCI (sMCI) from NC. However, this method is mainly focused on distinguishing AD from specific control groups

and does not address the MCI stage as a transitional phase. Meanwhile, the study in [8] developed a deep CNN-based pipeline designed to identify AD and categorize its various stages. This pipeline featured three separate deep CNN models, each with a unique configuration. The effectiveness of this approach was assessed using the OASIS dataset, but it is important to note that the validation was limited by the small size of the dataset, which included only 416 structural MRI (sMRI) scans.

In a recent advancement, researchers described in [9] developed a sophisticated deep CNN framework aimed at automating the segmentation of the hippocampus and classifying AD. This approach involves a two-step process: first, a deep CNN model is used to accurately segment the hippocampus, and then a 3D DenseNet model extracts critical image features for categorizing the disease. The method was tested with data from the ADNI database, including 97 AD patients, 233 individuals with mild cognitive impairment (MCI), and 119 healthy controls (NC). While the framework achieved a notable accuracy of 88.9% in distinguishing AD from NC, its utility is limited to these specific diagnostic categories and may not extend well to more complex classification scenarios.

Separately, the research presented in [10] proposed a machine learning-based algorithm for AD classification. This method combines Downsized Kernel Principal Component Analysis (DKPCA) with multiclass Support Vector Machines (SVM). However, the effectiveness of DKPCA is dependent on the quality and representativeness of the training dataset, which could impact its overall performance.

Additionally, the study in [11] introduced a functional MRI (fMRI)-based classification technique using the LeNet deep learning model. This method achieved a high accuracy of 96.86% in differentiating AD patients from normal controls (NC). Despite its success, this approach is limited to distinguishing between AD and NC, and does not address the identification of the intermediate MCI stage.

Lastly, the work described in [12] employed the Inception V3 model to analyze MRI images for AD detection. This strategy involved incorporating three advanced Inception blocks to improve the model's accuracy. Although the method reached an accuracy of 85.7%, it relies significantly on the appropriateness of the Inception V3 architecture for the task, which may restrict its effectiveness with more diverse or complex data distributions.

In [13], a novel approach combining CNN was developed for categorizing MRI images. This ensemble method utilized DenseNet architectures to achieve a high performance level, attaining an accuracy of 95.23%. Despite these promising results, the effectiveness of this approach could be impacted by the quality and configuration of the ensemble, and adapting it to different datasets may pose challenges.

In [14], a traditional machine learning framework was proposed for diagnosing Alzheimer's disease, using data from the ADNI dataset. The study compared six different data mining algorithms and highlighted the advantages of a generalized linear model (GLM). However, the approach's accuracy of 88.24% was relatively modest, given the complexity of the diagnostic task.

Separately, [15] presented a computational method for AD diagnosis that employed 3D brain MRI data. This technique involved a two-phase process: first, tissue segmentation was performed using a combination of CNN and Gaussian Mixture Models (GMM). The second phase used a hybrid model integrating extreme gradient boosting (XGBoost) and Support Vector Machines (SVM) for AD classification. While the combination of classifiers can address individual model limitations, the overall effectiveness of the approach may depend on the performance of each component.

The AD-126 dataset, which includes MRI scans of elderly individuals, presents more significant classification challenges due to age-related anatomical changes and pathologies. This complexity led to lower classification accuracy compared to the AD-86 dataset [15]. In [16], researchers introduced an innovative method for Alzheimer's Disease diagnosis that involved analyzing the shape of the hippocampus alongside anatomical biomarkers. This approach used a deep learning model integrating both structural MRI and clinical data to improve diagnostic accuracy. The model's ability to detect subtle hippocampal changes and their relationship with disease progression showed promise for early Alzheimer's detection. However, its effectiveness is heavily reliant on high-quality MRI data, which may not always be available, limiting its practical application.

In [17], a novel approach for Alzheimer’s Disease classification was proposed, featuring a 3D CNN that combined data from various neuroimaging modalities, including MRI and PET scans, through a multimodal feature fusion technique. This method enhanced the model's ability to differentiate between Alzheimer’s patients and healthy individuals by utilizing diverse data sources. Despite this, the integration of multiple modalities increased the complexity of the model, leading to higher computational requirements and the need for extensive training data.

The study presented in [18] developed a Temporal Convolutional Network (TCN) designed to capture temporal changes in brain imaging over time. This approach, by accounting for the progression of brain features, demonstrated improved accuracy in identifying different stages of Alzheimer’s Disease, which is crucial for tracking disease development. However, the TCN's performance can be affected by variations in imaging schedules and intervals, which may influence its ability to consistently capture temporal patterns.

In [19], the potential of combining multiple neuroimaging modalities for Alzheimer's diagnosis was explored using a deep learning framework that integrated structural MRI and PET scans. This multimodal approach enhanced the model's accuracy in distinguishing between Alzheimer's patients and healthy controls, highlighting the benefits of combining different data types. Nonetheless, integrating these modalities can complicate data processing and alignment, increasing computational demands.

The authors of [20] presented a robust CNN model tailored for Alzheimer's diagnosis using MR images. The model was designed to handle variations in data quality and patient demographics, improving its reliability in practical settings. While such models can reduce the impact of noisy or varied data, they may require complex tuning and validation to achieve optimal performance.

In paper [21], the authors explore early dementia detection challenges by developing an automated machine learning model for classifying cognitive states using MRI scans. They utilized 1167 scans to measure regional cortical thickness and applied various machine learning techniques, with the non-linear support vector machine (SVM) using a radial basis function kernel achieving the best performance at 75% accuracy. Despite its strengths, the approach may be limited by its focus on cortical thickness, which might miss other important biomarkers or structural changes. Additionally, the SVM's complexity can lead to high computational demands and reduced interpretability. The study's use of ten-fold cross-validation may not fully address potential overfitting issues due to variability in MRI data across dementia stages.

In paper [22], the authors advance Alzheimer's diagnosis by employing deep learning techniques, specifically 3D convolutional neural networks (3D-CNNs) combined with support vector machines (SVMs), and compare these with 2D-CNNs using MRI data. The 3D-CNN-SVM model showed superior performance with high accuracy for classifying normal controls, mild cognitive impairment, and Alzheimer's disease. This approach excels in avoiding manual feature extraction and is robust against variations in imaging protocols. However, its complexity may lead to high computational costs and a need for large training datasets. The model's effectiveness could also be influenced by the quality of the MRI data, and its implementation in clinical practice may require specialized knowledge.

Paper [23] addresses Alzheimer's diagnosis by integrating Diffusion Tensor Imaging (DTI) with Structural MRI, using a cross-modal transfer learning approach. Pre-trained models from Structural MRI are adapted for DTI Mean Diffusivity maps to address the challenge of limited training data and reduce overfitting, achieving an accuracy of 83.57%. The method improves classification by combining results from different classifiers. However, reliance on pre-trained models and cross-modal transfer may not fully overcome variability between imaging modalities or patient populations. Additionally, the approach's performance is contingent on the quality of the initial MRI data and the inherent limitations of deep learning models, such as computational demands and generalization issues.

In paper [24], the authors propose a method for early Alzheimer's diagnosis using advanced image processing techniques. They employ dual-tree complex wavelet transform (DTCWT) for feature extraction, followed by principal component analysis (PCA) for dimensionality reduction, and classify the results with a feed-forward neural network (FNN). This approach achieved a classification accuracy of 90.06%, with high sensitivity and specificity. However, the reliance on DTCWT and PCA may lead to complex feature representations and potential information loss during dimensionality reduction. The FNN's performance is dependent on the quality of feature extraction and training data, which may affect its applicability across different datasets and clinical conditions.

Research Gap: Despite significant advancements in the use of deep learning and machine learning techniques for the early detection and classification of AD, several research gaps remain that highlight the need for further innovation and improvement.

- ***Dependence on Labeled Data:*** Many existing methods, such as those discussed in [5] and [6], rely heavily on large, annotated datasets to achieve high classification accuracy. This dependency limits their applicability in scenarios where annotated data is scarce or expensive to obtain. For instance, the approach in [5] and [6] requires extensive labeled datasets to reach optimal performance, which may not always be available.
- ***Complexity and Computational Demand:*** Techniques like the one proposed in [17] and [19], which integrate multiple neuroimaging modalities or employ advanced deep learning frameworks, tend to have high computational requirements. These methods can be challenging to implement and require significant resources, making them less practical for widespread use in clinical settings.
- ***Limited Focus on MCI Stage:*** Several methods, such as the one described in [7] and [11], either focus primarily on distinguishing between AD and healthy controls or do not adequately address the transitional stage of Mild Cognitive Impairment (MCI). There is a need for approaches that more effectively integrate MCI as a critical transitional phase in the progression to AD.
- ***Performance Variability Across Datasets:*** Approaches like those in [12] and [23] exhibit performance variability depending on the dataset and quality of imaging data. Models that perform well on specific datasets may not

generalize effectively to others, highlighting a need for more robust methods that maintain high performance across diverse datasets.

- ***Integration and Adaptation Challenges:*** The methods discussed in [13] and [24] showcase high accuracy but often rely on complex feature extraction and dimensionality reduction techniques that can introduce information loss and require extensive tuning. Additionally, the integration of different imaging modalities can complicate data processing, as seen in [23].

Our proposed methodology addresses these gaps by leveraging a novel combination of feature extraction and classification techniques that are designed to reduce reliance on extensive labeled datasets, lower computational demands, and improve generalizability across different datasets. Additionally, our approach provides a more nuanced focus on the MCI stage, facilitating early detection and classification of AD in its transitional phases. By addressing these limitations, our methodology aims to offer a more practical and effective solution for early Alzheimer's detection and classification.

3. MATERIALS AND METHOD

A. DWT-LBP

The Discrete Wavelet Transform (DWT) combined with Local Binary Patterns (LBP) is a powerful technique used for texture feature extraction, particularly in the context of medical image analysis such as Alzheimer's disease detection. This method leverages the strengths of both DWT and LBP to capture intricate texture details and patterns within brain MRI images, which are often indicative of early pathological changes associated with the disease.

1. DWT for Multi-Resolution Analysis

DWT is a widely-used signal processing technique that decomposes an image into a set of frequency components, enabling the analysis of the image at multiple resolution levels. Unlike traditional Fourier Transform, which only provides frequency information without localization, DWT offers both spatial and frequency localization, making it highly suitable for analyzing localized changes in medical images.

The process begins by applying DWT to the brain MRI image, where the image is decomposed into different sub-bands: the approximation (low-frequency) sub-band and the detail (high-frequency) sub-bands. The approximation sub-band retains the coarse features of the image, capturing overall brightness and large structural details, while the detail sub-bands capture finer details, such as edges and textures, in different orientations (horizontal, vertical, and diagonal).

Mathematically, the DWT of a 2D image $I(x, y)$ can be expressed as:

$$W_{\psi}(j,k,l) = \sum_{x}\sum_{y} I(x,y)\psi_{j,k,l}(x,y)$$

(1)

Where $W_{\psi}(j,k,l)$ are the wavelet coefficients at scale j and location (k,l), and $\psi_{j,k,l}(x,y)$ is the wavelet function, which is a scaled and translated version of the mother wavelet $\psi(x,y)$.

The decomposition process continues iteratively on the approximation sub-band, further breaking it down into finer levels of detail. This hierarchical decomposition provides a multi-resolution representation of the image, making DWT particularly effective in identifying texture patterns that vary across different scales.

2. LBP for Micro-Texture Analysis

While DWT captures texture information across different scales, LBP is employed to extract micro-texture features from the image. LBP is a simple yet powerful texture operator that describes the local spatial structure of an image by comparing each pixel with its surrounding neighborhood.

For each pixel, LBP considers a circular neighborhood of P equally spaced pixels on a circle of radius R. The intensity of the center pixel is compared with each of its neighbors, and a binary pattern is generated by assigning a value of 1 if the neighbor's intensity is greater than or equal to the center pixel, and 0 otherwise. These binary values are then combined to form a binary number, which is converted into a decimal value representing the LBP code.

The LBP code for a pixel at position (x_c, y_c) is given by:

$$LBP_{P,R}(x_c, y_c) = \sum_{p=0}^{P-1} s(i_p - i_c) \times 2^p$$

(2)

Where i_p is the intensity of the neighboring pixel p, i_c is the intensity of the center pixel, and the function $s(x)$ is defined

as:

$$s(x) = \begin{cases} 1 & if\ x \geq 0 \\ 0 & if\ x < 0 \end{cases}$$

(3)

The resulting LBP codes for all pixels are compiled into a histogram, which serves as a compact representation of the texture features in the image. The histogram of LBP codes captures the distribution of local micro-textures across the entire image, making it a robust descriptor for texture classification.

3. Combining DWT and LBP for Enhanced Texture Feature Extraction

The integration of DWT and LBP enhances texture feature extraction by combining multi-resolution analysis with local texture pattern recognition. The process typically involves the following steps:

By combining DWT and LBP, a more comprehensive set of texture features is extracted from the MRI images. The DWT step decomposes the image into multiple sub-bands, each highlighting different levels of texture detail. The LBP is then applied to these sub-bands, particularly the detail sub-bands, to capture local texture patterns at each level of decomposition.

The process of combining DWT and LBP typically involves:

- ***DWT Decomposition:*** The MRI image undergoes DWT to produce sub-bands that separate different frequency components, focusing on both large-scale structures and fine details.
- ***LBP Computation:*** LBP is applied to the detail sub-bands generated by DWT. This step encodes local texture variations within these sub-bands, capturing micro-patterns that reflect subtle pathological changes.
- ***Feature Vector Construction:*** The LBP histograms derived from each sub-band are aggregated into a single feature vector. This vector encapsulates texture information from multiple scales and orientations, providing a rich representation of the image's textural characteristics.

B. Histogram of Oriented Gradients (HOG)

The HOG technique is a powerful method for structural feature extraction, particularly adept at capturing the shape and edge information crucial for distinguishing between different patterns or objects within an image. This method works by analyzing the directional changes in intensity within localized regions of the image, making it highly effective for highlighting structural details in complex images, such as those used in medical diagnostics.

Detailed process of HOG for structural feature extraction is represented as follows:

- ***Preprocessing and Gradient Computation:*** The process begins with preprocessing the input image, which might include steps like resizing and normalization to ensure uniformity across the dataset. Following this, the image gradients are computed. Gradients indicate the direction and rate of intensity change at each pixel and are derived using methods such as the Sobel operator. Specifically, horizontal (G_x) and vertical (G_y) gradients are calculated through convolution operations. The gradient magnitude $M(x, y)$ and orientation $\theta(x, y)$ at each pixel are then determined using the following formulas:

$$M(x, y) = \sqrt{G_x(x, y)^2 + G_x(x, y)^2}$$

(4)

$$\theta(x, y) = \arctan\left(\frac{G_y(x, y)}{G_x(x, y)}\right)$$

(5)

These calculations help to identify edges and their directions, which are key to understanding the structural features of the image.

- ***Division of Image into Cells:*** After gradient computation, the image is divided into small, non-overlapping regions called cells, typically sized 8×8 pixels. Within each cell, the orientations of the gradients are analyzed to create a histogram that represents the distribution of edge directions. Each bin in this histogram corresponds to a particular range of orientations, with the bin values representing the sum of the gradient magnitudes for pixels whose orientations fall within that range. This step captures the local structural information of the image, focusing on the distribution of edges in different directions.
- ***Feature Vector Construction:*** The histograms generated from all the cells are then concatenated to form a comprehensive feature vector. This vector encapsulates the structural characteristics of the image by reflecting the distribution of edge orientations across various parts of the image. Unlike methods that use block normalization,

here, the focus is on retaining the raw histogram data from each cell, allowing the feature vector to directly represent the localized structural features without additional normalization steps. This approach is particularly useful in scenarios where maintaining the original contrast and intensity variations is important for accurate analysis.

The HOG method, through its detailed analysis of gradient orientations, produces a feature vector that robustly represents the structural elements of an image. This feature vector is crucial for subsequent stages of image analysis, particularly in applications such as medical imaging, where detecting and analyzing fine structural details can be essential for early diagnosis and staging of diseases like Alzheimer's. By focusing on the edges and shapes within the image, HOG effectively captures the essential structural features needed for further processing and analysis.

C. Speeded-Up Robust Features (SURF)

The SURF technique is a widely utilized method for key point feature extraction, particularly valued for its speed and accuracy in detecting and describing local features within images. This approach is highly effective in capturing distinct, repeatable patterns that serve as key points, which are crucial for various image analysis tasks, including those in medical imaging where precise identification of structural variations is essential.

Detailed process of SURF for key point feature extraction is represented as follows:

- ***Preprocessing and Interest Point Detection:*** The process begins with preprocessing the input image, often involving steps such as converting the image to grayscale to simplify the analysis and reduce computational complexity. Following this, the SURF algorithm detects interest points, which are essentially locations in the image that exhibit high variability in intensity, making them distinct from their surroundings. SURF achieves this by using an approximation of the Hessian matrix, which helps identify points where the second-order intensity variations (or curvatures) are strong. The Hessian matrix is defined as:

$$H(x,y) = \begin{pmatrix} L_{xx}(x,y) & L_{xy}(x,y) \\ L_{xy}(x,y) & L_{yy}(x,y) \end{pmatrix}$$

(6)

Where $L_{xx}(x,y)$, $L_{yy}(x,y)$, and $L_{xy}(x,y)$ represent the second-order partial derivatives of the image intensity at point (x,y). Interest points are selected based on the determinant of this matrix, which indicates the presence of a blob-like structure.

- ***Scale-Space Representation:*** To ensure that key points are scale-invariant, SURF constructs a scale-space representation of the image. This is achieved by applying a series of filters at different scales to the image, effectively creating a pyramid of images where each level corresponds to a different scale. By detecting key points across these scales, SURF ensures that the extracted features are robust to changes in image size, making them applicable across different magnifications and resolutions.
- ***Orientation Assignment:*** Once the interest points are detected, the next step is to assign an orientation to each key point to ensure rotational invariance. SURF achieves this by computing the Haar wavelet responses in the neighborhood of each key point. These responses are summed up within a circular region around the key point, and the dominant orientation is determined by identifying the direction in which the sum of responses is maximal. This orientation is then assigned to the key point, allowing the feature descriptor to be invariant to image rotation.
- ***Descriptor Creation:*** After determining the location, scale, and orientation of each key point, the next step is to create a feature descriptor for each key point. The region around each key point is divided into smaller sub-regions, and within each sub-region, Haar wavelet responses are calculated. These responses are weighted by a Gaussian function centered on the key point, ensuring that responses closer to the key point have a higher influence on the descriptor. The wavelet responses are then used to form a feature vector that describes the local intensity pattern around the key point. This vector encapsulates the key point's structural properties, making it a robust representation for matching and comparison.
- ***Bag of Words (BoW) Technique:*** To handle the vast number of key points typically detected in an image, the SURF descriptors are further processed using the Bag of Words (BoW) technique. In BoW, the individual SURF descriptors are clustered into a set of visual words, each representing a group of similar key points. This clustering is usually done using algorithms like k-means. Once the visual words are defined, each image is represented as a histogram of visual words, where each bin in the histogram corresponds to the frequency of a particular visual word (i.e., key point type) in the image. This histogram serves as a compact feature vector that encapsulates the distribution of key point features within the image.
- ***Feature Vector Creation:*** After representing the image as a histogram of visual words through the BoW technique, the final step is to construct a feature vector that encapsulates the key point information of the entire image. This feature vector is a compact and discriminative representation of the image's content, where each element in the

vector corresponds to the frequency of a particular visual word (key point type). The dimensionality of this vector is determined by the number of clusters (visual words) used in the BoW model.

The application of SURF combined with the Bag of Words technique produces a highly informative feature vector that captures the essential key point characteristics of the image. This vector, reflecting the frequency and type of detected key points, is crucial for further analysis in scenarios where precise and detailed image representation is needed, such as in the early detection and staging of diseases like Alzheimer's. By focusing on the identification and categorization of key points, this method enables a comprehensive understanding of the image's structural content, facilitating the extraction of meaningful insights in subsequent stages of analysis.

D. Enhanced Snake Optimization (ESO)

ESO is an advanced metaheuristic optimization technique inspired by the behavior of snakes in nature. This method is particularly useful for optimizing complex functions, such as those involved in training neural networks. The ESO algorithm seeks to improve the performance of a neural network by fine-tuning its parameters, such as weights and biases, to achieve better accuracy and generalization.

- ***Inspiration and Mechanism:*** ESO draws inspiration from the way snakes move and hunt, employing a combination of exploration and exploitation strategies. The optimization process mimics a snake's movement in search of prey, balancing between searching for new optimal regions (exploration) and refining existing solutions (exploitation). This dual approach enables ESO to efficiently navigate the search space, avoiding local optima while converging on a global optimum.
- ***Initialization:*** The optimization process begins by initializing a population of candidate solutions, which are akin to the positions of multiple snakes within the search space. Each candidate solution represents a potential set of neural network parameters. These initial solutions are typically generated randomly to ensure a broad coverage of the search space.
- ***Position Update Strategy:*** The core of the ESO algorithm lies in its position update strategy. In each iteration, the position of each candidate solution (snake) is updated based on the collective behavior of the population and the individual snake's experience. This update is governed by mathematical equations that simulate the serpentine motion, allowing the algorithm to traverse the search space smoothly. The updated positions are influenced by factors such as the best-known solution, neighboring solutions, and random perturbations that inject diversity into the search process.
- ***Fitness Evaluation:*** After updating the positions, the fitness of each candidate solution is evaluated. In the context of neural network optimization, this fitness function is typically the network's performance on a validation dataset, measured by a metric like accuracy or loss. The better the network's performance, the higher the fitness of the corresponding candidate solution.
- ***Selection of the Best Solution:*** As the ESO algorithm iterates, it continually refines the population of solutions, discarding less effective candidates and retaining those that lead to better network performance. The algorithm keeps track of the best solution found so far, which is updated as better solutions are discovered.
- ***Termination and Optimization Outcome:*** The ESO process continues for a predetermined number of iterations or until a convergence criterion is met. The final output of the ESO algorithm is the set of neural network parameters that yielded the highest fitness, representing the optimal configuration for the given problem.

ESO is crucial for enhancing the performance of neural networks by systematically searching for the best possible set of parameters. This optimization process ensures that the neural network is fine-tuned to provide the most accurate predictions, making it a vital component in advanced diagnostic frameworks, such as those used for Alzheimer's disease detection.

4. PROPOSED METHODOLOGY

The proposed methodology for Alzheimer's disease detection is illustrated in Figure 1, begins with the acquisition of MRI brain images from a benchmark database. These images serve as the foundation for the subsequent analytical processes. After acquisition, the images undergo contrast enhancement using CLAHE, which enhances the visibility of critical features by improving image contrast.

Following this, the framework employs multiple feature extraction techniques to capture various aspects of the brain's structure and texture. DWT combined with LBP is used for detailed texture analysis, capturing microstructural changes. Simultaneously, HOG is utilized for structural feature extraction, highlighting significant shape-related features. Additionally, SURF with BoW technique is implemented for key point feature extraction, effectively capturing localized patterns within the images. These extracted features are then integrated into a combined feature vector, which undergoes feature selection using NCA. The selected features are subsequently classified using a combination of SVM, KNN, and ESO-optimized neural network. The final step in the methodology involves performance evaluation, where the accuracy,

sensitivity, specificity, and other relevant metrics are assessed to validate the effectiveness of the proposed framework in detecting and staging Alzheimer's disease. The detailed description of each of these steps is provided in the following sub-sections.

A. Image Acquisition

The initial phase of the proposed Alzheimer's disease detection framework is the acquisition of brain MRI images from a well-established, publicly accessible database. This empirical research centers on the examination of T1-weighted cross-sectional MR brain scans, with data specifically sourced from the Open Access Series of Imaging Studies (OASIS) repository. The OASIS database offers a comprehensive collection of high-resolution MRI scans, covering various stages of cognitive decline, including normal aging, mild cognitive impairment (MCI), and Alzheimer's disease.

The images are typically stored in the Digital Imaging and Communications in Medicine (DICOM) format, which is advantageous because it retains both the imaging data and extensive metadata. This metadata includes crucial details about the patient, the imaging equipment used, and specific parameters of the MRI scan, all of which are vital for subsequent analysis stages.

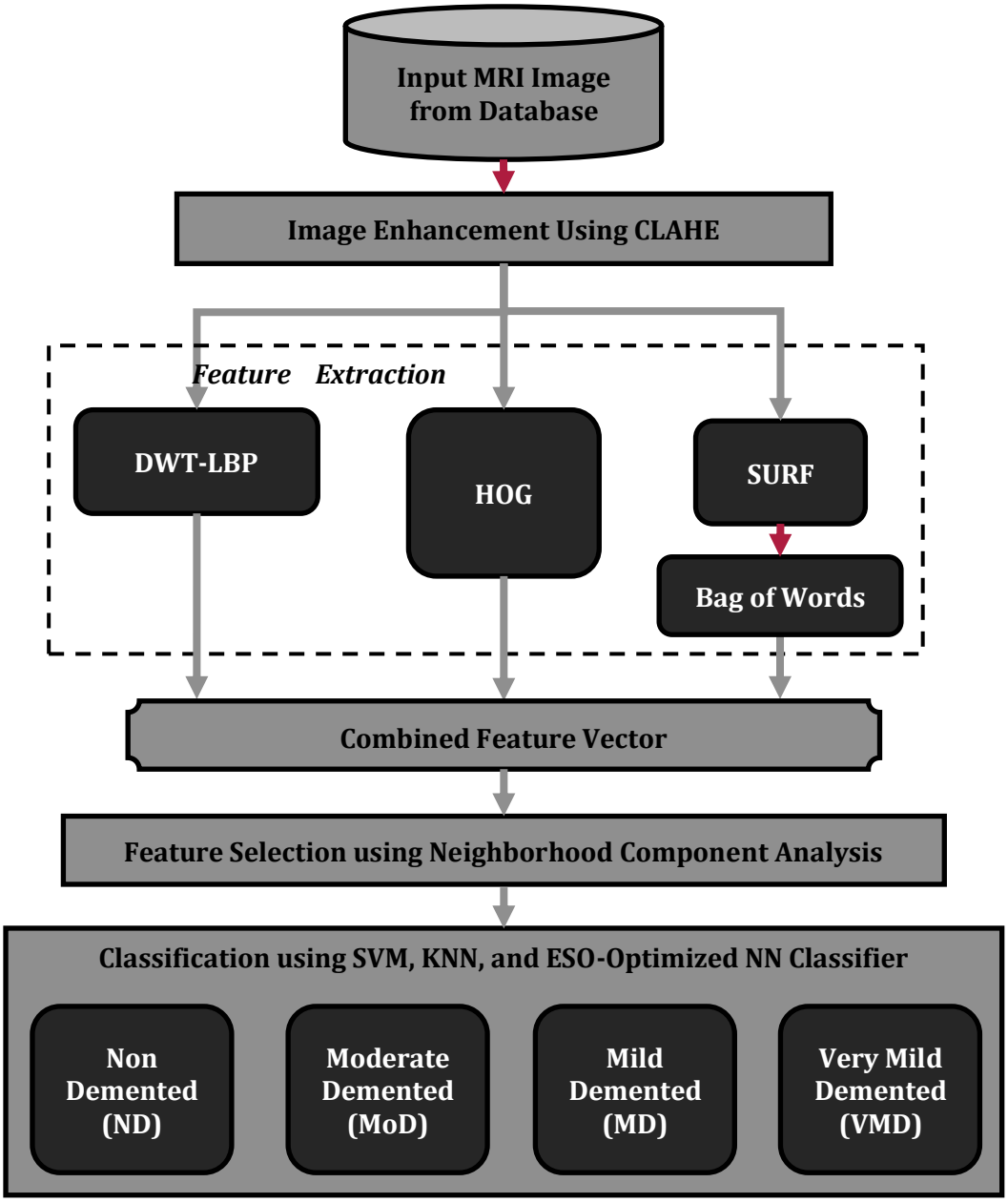

Figure 1: Block diagram for proposed Alzheimer's disease detection

Mathematically, the acquisition process can be represented as follows:

Given a dataset D consisting of N T1-weighted MRI scans, each image I_i is retrieved as:

$$I_i = DICOM(ScanID_i, Metadata_i) \quad for\ i = 1,2,\dots,N$$

(7)

Where:

- I_i represents the i^{th} MRI image.
- $ScanID_i$ is the unique identifier for each scan in the OASIS database.
- $Metadata_i$ includes essential scan details like patient information, imaging parameters, and equipment specifics.

The high-quality and disease-relevant images acquired from the OASIS database form the foundational input for the diagnostic framework, ensuring that the subsequent processes of feature extraction and analysis are grounded on robust and accurate data.

B. Contrast Enhancement using CLAHE

Following the image acquisition, the next critical step in the proposed methodology is the enhancement of image contrast, which is achieved using Contrast Limited Adaptive Histogram Equalization (CLAHE). CLAHE is an advanced version of the traditional histogram equalization technique, designed specifically to improve local contrast while avoiding the over-amplification of noise that can occur with standard methods.

CLAHE operates by dividing the image into smaller, non-overlapping regions called "tiles." Within each tile, the contrast is enhanced by redistributing the intensity values based on the local histogram, but with a limitation imposed on the contrast to prevent noise amplification. The enhanced tiles are then seamlessly combined using bilinear interpolation to produce the final contrast-enhanced image.

Mathematically, the process can be represented as follows:

Tiling of the Image: The image $I_{orig}(i,j)$ is partitioned into small, non-overlapping regions of size $S \times S$. Each tile $T_{i,j}$ is processed individually for contrast enhancement.

$$I_{orig}(i,j) \rightarrow \{T_{p,q}\}$$

(8)

With $p = 1,2,\dots,\frac{M}{S}\ and\ q = 1,2,\dots,\frac{N}{S}$

Here, $T_{p,q}$ denotes the tile located at position (p,q), and M and N are the dimensions of the image.

Histogram Computation and Clipping: For each tile $T_{p,q}$, compute the histogram $H_{p,q}(k)$ for pixel intensities k. This histogram is then clipped at a threshold L_{clip} to prevent excessive contrast enhancement and reduce noise.

$$H_{p,q}^{clipped}(k) = \min\left(H_{p,q}(k), L_{clip}\right)$$

(9)

The clipped histogram is then normalized:

$$H_{p,q}^{norm}(k) = \frac{H_{p,q}^{clipped}(k)}{\sum_k H_{p,q}^{clipped}(k)}$$

(10)

Cumulative Distribution Function (CDF) Calculation: Compute the CDF from the normalized histogram to map the intensity values within the tile.

$$CDF_{p,q}(k) = \sum_{l=0}^{k} H_{p,q}^{norm}(l)$$

(11)

Intensity Mapping: Map each pixel intensity $I_{orig}(i,j)$ in the tile to a new intensity value based on the CDF:

$$I'_{p,q}(i,j) = CDF_{p,q}\left(I_{orig}(i,j)\right)$$

(12)

Tile Merging: The contrast-enhanced tiles are merged into the final image using interpolation to ensure smooth transitions between tiles. The final enhanced image $I_{enhanced}(i,j)$ is obtained by combining these tiles:

$$I_{enhanced}(i,j) = \text{Interpolate}\left(T'_{p,q}(i,j)\right)$$

(13)

CLAHE enhances image contrast by local histogram equalization, clipping, and redistributing intensity values within tiles, followed by smoothing through interpolation. This process makes fine details more visible and improves subsequent feature extraction stages.

C. Features Extraction

ABCD.

Feature extraction involves identifying and quantifying important characteristics of images that are relevant for analysis. Here, we discuss various feature extraction methods to capture textural, and structural, and key point based features in images.

1. DWT-LBP Based Feature Extraction

In this approach, texture and structural features are extracted by integrating DWT with LBP, providing a detailed representation of the image's multi-resolution texture characteristics.

Discrete Wavelet Transform (DWT): DWT is employed to decompose the image into various frequency components. This decomposition captures different levels of detail across multiple scales, providing a nuanced view of the image's texture. The image is divided into several sub-bands representing various frequency ranges, including:

- ***Approximation Sub-Band (LL):*** Contains the low-frequency information and represents the coarse details.
- ***Detail Sub-Bands (LH, HL, and HH):*** Contain high-frequency information, capturing edges and finer texture details.

These sub-bands are used to analyze features at different resolutions.

Local Binary Patterns (LBP): LBP is applied to the detail sub-bands obtained from DWT. This method analyzes local texture patterns by comparing each pixel with its neighboring pixels. The local texture features are encoded into binary patterns which are then represented as histograms. For each pixel, the LBP is computed based on a circular neighborhood of pixels:

$$LBP_{P,R}(x,y) = \sum_{p=0}^{P-1} s(I_p - I_c) \cdot 2^p$$

(14)

Where I_p is the intensity of the p^{th} neighbor, I_c is the intensity of the center pixel, and $s(x)$ is a threshold function that outputs 1 if $x \geq 0$ and 0 otherwise.

Integration of DWT and LBP: After applying DWT, the image is decomposed into several sub-bands. LBP histograms are computed for each of the detail sub-bands to capture local texture features. The combined feature vector is created by concatenating these histograms:

$$F_{DWT-LBP} = [Hist_{LH}, Hist_{HL}, Hist_{HH}]$$

(15)

Where $Hist_{LH}$, $Hist_{HL}$, and $Hist_{HH}$ are the histograms of LBP codes for the LH, HL, and HH sub-bands respectively.

This combined approach allows for capturing both the global texture patterns and local micro-textures, providing a comprehensive feature representation for subsequent analysis.

2. HOG for Structural Feature Extraction

The HOG technique is utilized for extracting structural features from images by analyzing the distribution of gradient orientations. This method is particularly effective for capturing the shape and edge information crucial for image analysis, which is instrumental in distinguishing structural patterns within medical images.

Gradient Computation: The first step in HOG involves computing the gradient of the image to detect edges and the direction of intensity changes. The gradients are calculated using convolution operations with Sobel filters to determine the gradient magnitude and orientation at each pixel. For an image $I(x,y)$, the gradients are computed as follows:

$$G_x(x,y) = I(x+1,y) - I(x-1,y)$$

(16)

$$G_y(x,y) = I(x,y+1) - I(x,y-1)$$

(17)

The gradient magnitude $M(x,y)$ and orientation $\theta(x,y)$ are then derived using:

$$M(x,y) = \sqrt{G_x(x,y)^2 + G_x(x,y)^2}$$

(18)

$$\theta(x,y) = \arctan\left(\frac{G_y(x,y)}{G_x(x,y)}\right)$$

(19)

Cell Division: The image is divided into small, non-overlapping regions called cells, typically of size 8×8 pixels. For each cell, a histogram of gradient orientations is computed. The orientation bins in the histogram are generally defined with a fixed number of bins, such as 9, each covering an angular range of 20 degrees.

Orientation Bin Calculation: Each gradient in the cell contributes to the histogram based on its orientation. The histogram bin corresponding to the gradient's orientation is incremented by the magnitude of the gradient. The orientation bin value $H_{c,b}$ for a cell c and bin b is calculated as:

$$H_{c,b} = \sum_k M(x_k, y_k) \cdot w_b \theta(x_k, y_k)$$

(20)

Where $w_b(\theta)$ is a weight assigned to the gradient based on how closely the gradient orientation matches the bin center, and (x_k, y_k) are the coordinates of the pixels within the cell.

Block Normalization: To enhance the robustness of the descriptors against variations in illumination and contrast, cells are grouped into larger blocks (e.g., 2×2 cells), and the histograms of these cells are normalized. The normalized feature vector F_{block} for a block is given by:

$$F_{block} = \frac{H_{block}}{\sqrt{\|H_{block}\|^2 + \epsilon^2}}$$

(21)

Where H_{block} is the concatenated histogram vector of all cells within the block, and ϵ is a small constant to avoid division by zero.

Feature Vector Construction: The final HOG feature vector is constructed by concatenating the normalized histograms from all blocks. This feature vector captures the distribution of gradient orientations across the image, reflecting the structural and textural details.

$$F_{HOG} = \left[F_{block_1}, F_{block_2}, \ldots, F_{block_N}\right]$$

(22)

Where F_{block_i} represents the normalized feature vector of the i^{th} block, and N is the total number of blocks in the image.

This approach effectively captures the structural features by analyzing the distribution and orientation of gradients, providing a robust representation of the image's shape and edge information essential for subsequent analysis.

3. SURF with BoW for Key Point Feature Extraction

The SURF combined with the Bag of Words (BoW) technique is used for extracting and representing key points in images. This method is effective for capturing distinctive local features and categorizing them into a histogram-based representation, which is particularly useful in image analysis tasks.

Key Point Detection and Description:

- ***Interest Point Detection:*** The SURF algorithm detects interest points, which are significant locations in the image characterized by high contrast or distinctive structures. This is achieved using an approximation of the Hessian matrix to identify blob-like structures.

The Hessian matrix $H(x, y)$ at a point (x, y) is defined as:

$$H(x,y) = \begin{pmatrix} L_{xx}(x,y) & L_{xy}(x,y) \\ L_{xy}(x,y) & L_{yy}(x,y) \end{pmatrix}$$

(23)

Here, $L_{xx}(x, y)$ and $L_{yy}(x, y)$ are the second-order partial derivatives in the x and y directions, respectively, and $L_{xy}(x, y)$ is the mixed partial derivative.

- ***Descriptor Computation:*** For each detected key point, a feature descriptor is created to represent the local texture around the point. This involves computing Haar wavelet responses in a neighborhood around each key point. The responses are weighted by a Gaussian function to emphasize regions closer to the key point.

The descriptor vector D for a key point is computed as:

$$D_i = \sum_{k \in region_i} w_k \cdot R_k$$

(24)

Where R_k denotes the Haar wavelet response in the k^{th} sub-region, and w_k is the weight assigned based on the Gaussian function.

Bag of Words (BoW) Representation

- ***Feature Vector Formation:*** To manage the extensive number of key points and their descriptors, the BoW approach is applied. This involves clustering the SURF descriptors into a set of visual words using a clustering algorithm like k-means.

Let V denote the visual vocabulary, consisting of K clusters, where each cluster represents a visual word. The clustering assigns each key point descriptor to the nearest cluster center:

$$Cluster(D_i) = \arg\min_{c \in V} \|D_i - C_c\|$$

(25)

Here, C_c represents the centroid of cluster c, and $\|\cdot\|$ denotes the Euclidean distance.

- ***Histogram Creation:*** Each image is then represented as a histogram of visual words, where each bin corresponds to the frequency of a particular visual word in the image:

$$H_j = \sum_{i \in image} count(D_i \in cluster_j)$$

(26)

Here, H_j represents the count of descriptors assigned to the j^{th} cluster, and $count(\cdot)$ denotes the counting function.

Feature Vector Construction

- ***Concatenation of Histograms:*** The final feature vector for each image is constructed by concatenating the histograms from all clusters. This vector provides a compact and discriminative representation of the key points within the image:

$$F_{SURF} = [H_1, H_2, \ldots, H_K]$$

(27)

In this equation, H_K denotes the histogram of the k^{th} visual word, and K is the total number of clusters.

The SURF with BoW approach provides a robust and efficient way to extract and represent key point features from images. By summarizing the distribution of these features into a histogram format, this method facilitates effective image classification and retrieval.

4. Combined Feature Vector

The combined feature vector integrates the diverse and complementary feature sets extracted through DWT-LBP, HOG, and SURF with BoW techniques. This fusion of features creates a more comprehensive and discriminative representation of the image, enhancing the ability of the model to capture subtle and complex patterns relevant to tasks such as Alzheimer's disease detection.

- ***DWT-LBP Feature Vector:*** The DWT-LBP captures multi-resolution texture features from the image. The feature vector derived from this method is denoted as:

$$F_{DWT-LBP} = [f_1^{DWT-LBP} - f_2^{DWT-LBP}, \dots, f_m^{DWT-LBP}]$$

(28)

Where m represents the number of features extracted from the DWT-LBP method.

- ***HOG Feature Vector:*** The HOG extracts structural features by analyzing the distribution of gradient orientations across localized regions of the image. The feature vector from HOG is represented as:

$$F_{HOG} = [f_1^{HOG} - f_2^{HOG}, \dots, f_n^{HOG}]$$

(29)

Where n represents the number of features obtained from the HOG method.

- ***SURF with BoW Feature Vector:*** The SURF combined with the BoW technique captures key point-based features and summarizes them into a histogram of visual words. The feature vector derived from this process is denoted as:

$$F_{SURF} = [f_1^{SURF} - f_2^{SURF}, \dots, f_p^{SURF}]$$

(30)

Where p is the number of histogram bins or clusters used to represent the BoW feature.

- ***Formation of the Combined Feature Vector:*** The combined feature vector is created by concatenating the individual feature vectors obtained from DWT-LBP, HOG, and SURF with BoW methods. This concatenated vector, denoted as $F_{combined}$, is formed as follows:

$$F_{combined} = [F_{DWT-LBP}, F_{HOG}, F_{SURF}]$$

(31)

Mathematically, this can be expressed as:

$$F_{combined} = [f_1^{DWT-LBP}, \dots, f_m^{DWT-LBP}, f_1^{HOG}, \dots, f_n^{HOG}, f_1^{SURF}, \dots, f_p^{SURF}]$$

(32)

Where the total length of the combined feature vector $F_{combined}$ is $m + n + p$.

By integrating the features from DWT-LBP, HOG, and SURF with BoW, the combined feature vector $F_{combined}$ encapsulates a rich set of texture, structural, and key point-based information. This comprehensive representation is highly beneficial for tasks requiring detailed and nuanced image analysis, such as medical image classification.

D. NCA-Based Feature Selection

NCA is employed as a feature selection technique to refine the combined feature vector by identifying and retaining the most discriminative features for the classification task. NCA is particularly effective because it focuses on improving the performance of a nearest neighbor classifier, optimizing the selection of features that enhance class separability.

1. Objective of NCA

The primary objective of NCA is to learn a transformation matrix that maximizes the classification accuracy by optimizing the distance between data points from the same class while maximizing the distance between points from different classes. Given a dataset with the combined feature vector $F_{combined}$ and corresponding class labels, NCA learns a linear transformation that projects the data into a lower-dimensional space where the discriminative power of the features is maximized.

2. Mathematical Formulation

Let $X \in \mathbb{R}^{d \times N}$ represent the combined feature matrix, where d is the total number of features (i.e., the length of $F_{combined}$) and N is the number of samples. The goal of NCA is to find a transformation matrix $A \in \mathbb{R}^{d' \times d}$, where $d' < d$, that maps the original feature space X to a new space $Z = AX$.

The probability p_{ij} of a sample x_i choosing x_j as its neighbor under this transformation is given by:

$$p_{ij} = \frac{\exp\left(-\|A(x_i - x_j)\|^2\right)}{\sum_{k \neq i} \exp(-\|A(x_i - x_k)\|^2)}$$

(33)

Where $\|\cdot\|$ denotes the Euclidean norm. The objective is to maximize the expected number of correctly classified points by maximizing the following function:

$$L(A) = \sum_{i=1}^{N} \sum_{\substack{j=1 \\ y_i = y_j}}^{N} p_{ij}$$

(34)

Here, y_i and y_j represent the class labels of the samples x_i and x_j. The optimization of $L(A)$ helps in determining the optimal transformation matrix A, which in turn identifies the most important features.

3. Feature Selection Process

Once the optimal transformation matrix A is obtained, the transformed feature set $Z = AX$ is used to select the top k features that contribute most significantly to the classification task. The selected feature vector $F_{selected}$ is then formed by retaining only these top k features from the combined feature vector $F_{combined}$.

Mathematically, the selected feature vector can be represented as:

$$F_{selected} = [z_1, z_2, \dots, z_k]$$

(35)

Where z_i corresponds to the most significant features as determined by the NCA.

4. Outcome of NCA-Based Feature Selection

The NCA-based feature selection process results in a refined and reduced feature vector $F_{selected}$, which preserves the most discriminative characteristics of the original dataset. This selected feature set is optimized for classification tasks, reducing the dimensionality of the input data while maintaining or even enhancing the model's performance. By focusing on the most relevant features, this method improves computational efficiency and accuracy in subsequent classification stages.

E. Classification

Classification is the final stage in the process of analyzing MRI images for Alzheimer's disease detection. After feature extraction and selection, the selected feature set $F_{selected}$ is used to classify the images into relevant categories. These classification techniques—SVM, KNN, and ESO-optimized Neural Network—each offer distinct advantages for the task of Alzheimer's disease detection. SVM provides a robust linear or non-linear decision boundary, KNN offers a simple and intuitive approach based on proximity, and the ESO-optimized Neural Network leverages advanced optimization to enhance the model's learning capability. Combining these classifiers or selecting the most suitable one based on the problem characteristics can significantly improve the accuracy and reliability of the Alzheimer's detection system.

1. Support Vector Machine (SVM)

SVM is a powerful supervised learning algorithm that is widely used for classification tasks. SVM aims to find the optimal hyperplane that separates different classes in the feature space. The optimal hyperplane is defined as the one that maximizes the margin, i.e., the distance between the hyperplane and the closest data points of any class, known as support vectors.

Given a set of training data $\{z_i, y_i\}_{i=1}^{N}$, where $z_i \in \mathbb{R}^{d'}$ represents the selected feature vector for the i^{th} sample and $y_i \in \{-1,1\}$ is the class label, SVM attempts to find a hyperplane described by the equation:

$$w^T z + b = 0$$

(36)

Where w is the weight vector perpendicular to the hyperplane, and b is the bias term. The decision function for classifying a new sample z is given by:

$$f(z) = \text{sign}(w^T z + b)$$

(37)

To find the optimal hyperplane, SVM solves the following optimization problem:

$$\min_{w,b} \frac{1}{2} \|w\|^2$$

(38)

Subject to the constraints:

$$y_i(w^T z_i + b) \geq 1 \quad \forall i$$

(39)

Soft Margin and Kernel Trick: In cases where data is not linearly separable, SVM introduces slack variables ξ_i to allow for some misclassifications, leading to a "soft margin" SVM. The optimization problem is modified as:

$$\min_{w,b,\xi} \frac{1}{2}\|w\|^2 + C\sum_{i=1}^{N} \xi_i$$

(38)

Subject to:

$$y_i(w^T z_i + b) \geq 1 - \xi_i, \quad \xi_i \geq 0 \quad \forall_i$$

(39)

Where C is a regularization parameter controlling the trade-off between maximizing the margin and minimizing the classification error.

When the data is not linearly separable in the original feature space, SVM can employ the "kernel trick" to map the data into a higher-dimensional space where a linear separation is possible. Common kernels include:

- Linear Kernel: $K(z_i, z_j) = z_i^\top z_j$
- Polynomial Kernel: $K(z_i, z_j) = (z_i^\top z_j + 1)^p$
- Radial Basis Function (RBF) Kernel: $K(z_i, z_j) = \exp\left(-\gamma\|z_i - z_j\|^2\right)$

SVM in Alzheimer's Detection: In this context, the selected feature vector $F_{selected}$ is used as input to the SVM classifier. The SVM is trained to distinguish between Alzheimer's and non-Alzheimer's cases based on the extracted features. The optimal hyperplane or decision boundary learned by the SVM model is then used to classify new MRI images.

2. K-Nearest Neighbors (KNN)

KNN is a simple, yet effective, non-parametric classification algorithm. It operates based on the idea that similar data points tend to be close to each other in the feature space. KNN classifies a given sample based on the majority class among its k-nearest neighbors.

For a given sample z_{test}, the KNN algorithm calculates the distance between z_{test} and all the training samples z_i in the feature space $\mathbb{R}^{d'}$. A common distance metric used is the Euclidean distance:

$$D(z_{test}, z_i) = \sqrt{\sum_{j=1}^{d'} (z_{test,j} - z_{i,j})^2}$$

(40)

where $z_{test,j}$ and $z_{i,j}$ are the j^{th} components of the test sample and the i^{th} training sample, respectively.

After computing the distances, KNN identifies the k closest training samples to z_{test}. The test sample is then classified according to the majority class among these k-nearest neighbors. The classification label y_{test} is determined as:

$$y_{test} = \text{mode}\{(y_i : z_i \in \mathcal{N}_k(z_{test}))\} \quad (41)$$

Where $\mathcal{N}_k(z_{test})$ represents the set of the k-nearest neighbors of z_{test}.

Choice of k: The parameter k significantly impacts the performance of the KNN classifier. A small k makes the classifier sensitive to noise, while a large k may smooth out decision boundaries excessively. The optimal value of k is typically determined through cross-validation.

KNN in Alzheimer's Detection: For Alzheimer's disease detection, KNN uses the selected feature vector $F_{selected}$ as input. The algorithm classifies MRI images by comparing them with the stored feature vectors from the training set. KNN is particularly effective when the dataset is well-labeled and the decision boundary between classes is complex.

3. ESO-Optimized Neural Network

Enhanced Snake Optimization (ESO) is a metaheuristic optimization algorithm inspired by the movement and hunting strategies of snakes. ESO is used to optimize the parameters of a Neural Network (NN) to achieve high classification accuracy

in complex tasks such as Alzheimer's disease detection.

Neural Network Architecture: A typical neural network used in this context consists of an input layer, multiple hidden layers, and an output layer. The number of neurons in the input layer corresponds to the dimensionality of the feature vector $F_{selected}$, and the output layer typically consists of a single neuron for binary classification (e.g., Alzheimer's vs. non-Alzheimer's).

The forward pass of a neural network is defined as:

$$h^{(l+1)} = \sigma\left(W^{(l)}h^{(l)} + b^{(l)}\right) \quad (42)$$

Where $h^{(l)}$ is the activation of the l^{th} layer, $W^{(l)}$ is the weight matrix, $b^{(l)}$ is the bias vector, and $\sigma(\cdot)$ is the activation function (e.g., ReLU, sigmoid). The final output is passed through a softmax or sigmoid function to obtain a probability score for each class.

ESO for Neural Network Optimization: ESO is employed to optimize the weights $W^{(l)}$ and biases $b^{(l)}$ of the neural network. ESO mimics the natural hunting strategy of snakes, balancing exploration and exploitation to find the global optimum of the network's parameter space.

Position Update Strategy in ESO: The position of each snake (candidate solution) is updated using a combination of exploration and exploitation strategies. The position $p^{(t+1)}$ at iteration $t+1$ is updated as:

$$p^{(t+1)} = p^{(t)} + \alpha \cdot Exploration\left(p^{(t)}\right) + \beta \cdot Exploitation\left(p^{(t)}\right) \quad (43)$$

Where α and β are weights controlling the contribution of exploration and exploitation, respectively. Exploration helps the algorithm search in new regions of the parameter space, while exploitation refines the solution by searching in the vicinity of promising regions.

Fitness Evaluation: The fitness of each snake (candidate solution) is evaluated based on the classification accuracy of the neural network on the validation set. The objective is to minimize the classification error, leading to the following fitness function:

$$Fitness(p) = \frac{1}{N_{val}} \sum_{i=1}^{N_{val}} \mathbb{I}(y_i \neq \hat{y}_i) \quad (44)$$

Where N_{val} is the number of validation samples, y_i is the true label, $\hat{y}_i$ is the predicted label, and $\mathbb{I}$ is the indicator function.

ESO-Optimized Neural Network in Alzheimer's Detection: In the context of Alzheimer's disease detection, the ESO algorithm optimizes the neural network to effectively classify MRI images based on the selected features $F_{selected}$. The ESO-optimized neural network is expected to outperform traditional optimization methods by efficiently exploring the parameter space and avoiding local minima, thereby achieving higher classification accuracy.

ESO-Optimized Neural Network Pseudo-Code:

```
# Initialization
Initialize NN_parameters
Initialize ESO_parameters
# Data Preparation
Load_and_preprocess_data()
# ESO Algorithm
Initialize_population()
While not termination_condition:
    For each individual in population:
        Set_NN_parameters(individual)
        Train_NN_on_training_data()
        Evaluate_fitness(individual)
    Select_best_individuals()
    Perform_crossover()
```

Apply_mutation()

Replace_worst_individuals()

 # Final Training

Select_best_individual()

Set_NN_parameters(best_individual)

Train_NN_on_full_training_data()

 # Testing

Evaluate_NN_on_test_data()

Output_final_model_and_metrics()

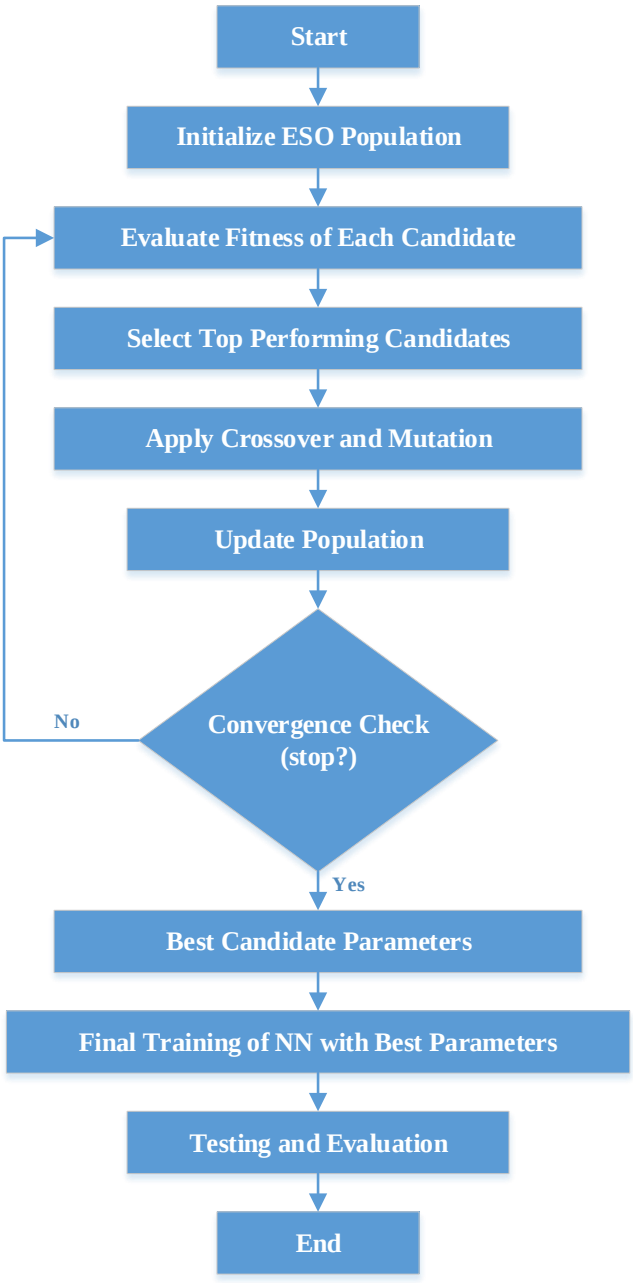

Figure 2: Flow diagram for ESO optimization of Neural Network

Figure 2 shows the ESO optimization process for Neural Networks. It begins with initializing a population of candidate solutions, each representing different sets of NN parameters. The fitness of each candidate is evaluated using validation data to determine how well they perform. The top-performing candidates are then selected and subjected to genetic operators, such as crossover and mutation, to generate new candidates. The population is updated with these new solutions, and a convergence check is performed to see if the optimization process should stop. If the process has converged, the best candidate parameters are chosen. These optimal parameters are then used to train the Neural Network, followed by testing and evaluating its performance on test data. The process concludes once the NN has been fully optimized and assessed.

5. RESULTS AND DISCUSSION

A. Dataset

This study focuses on analyzing publicly available T1-weighted MR brain scans, specifically utilizing data from the OASIS repository from Kaggle [25]. The latest version, OASIS-3, provides a comprehensive collection of neuroimaging data valuable for research purposes. This updated database includes longitudinal imaging data, clinical assessments, cognitive evaluations, and biomarker information related to normal aging and Alzheimer's disease.

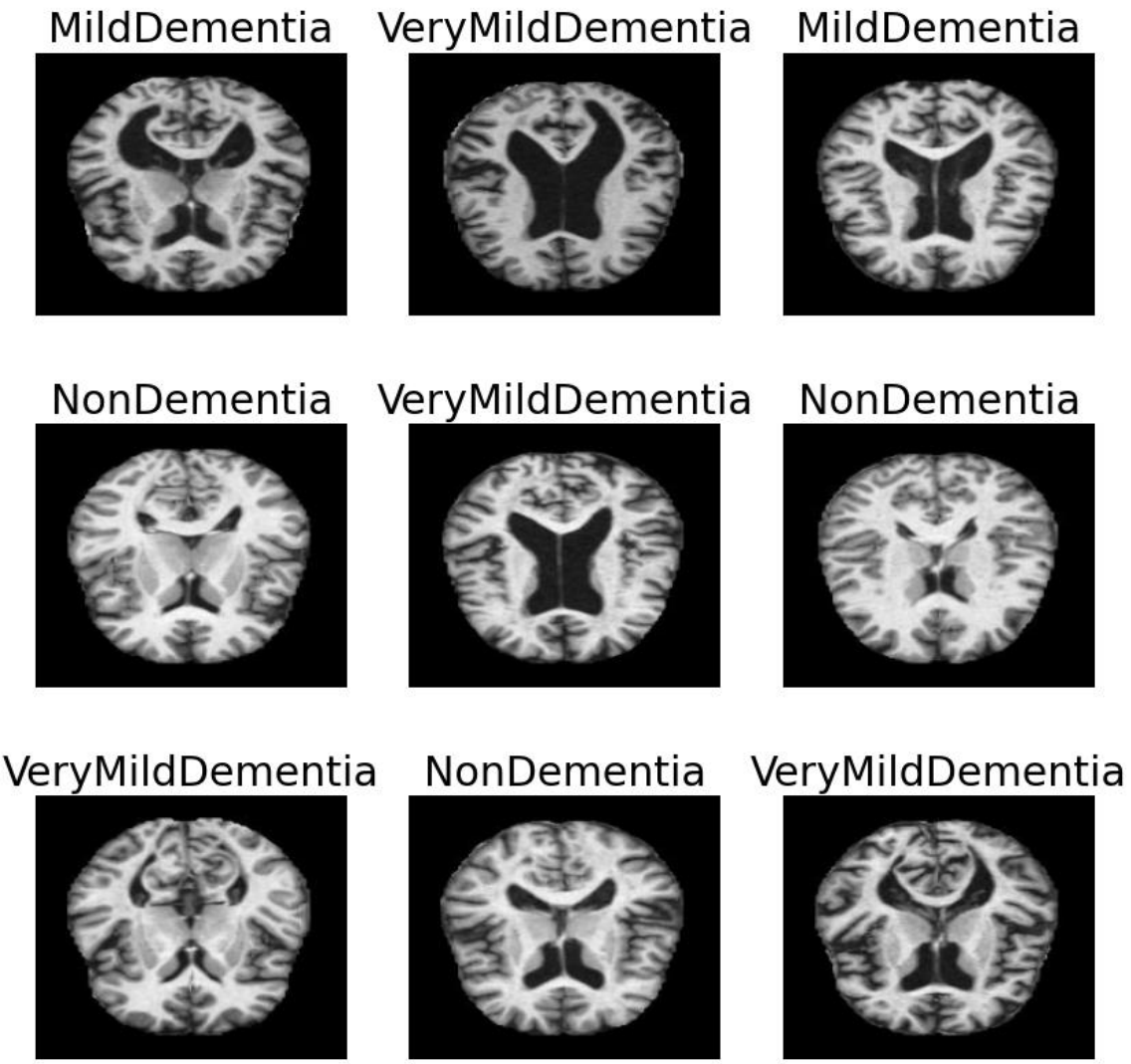

Figure 3: Sample image from OASIS-3 database [25]

The dataset used in this research comprises a total of 6,400 MR brain images, which are divided into four categories based on the severity of Alzheimer's disease. These categories are labeled as Non Dementia (ND), Moderate Dementia (MoD), Mild Dementia (MD), and Very Mild Dementia (VMD), each representing different stages of disease progression. Specifically, the dataset distribution includes 3,200 images for ND, 64 for MoD, 896 for MD, and 2,240 for VMD.

For model development and evaluation, the dataset is split into separate training and testing subsets. Leveraging this extensive

dataset, the research aims to create and assess algorithms designed to detect and stage Alzheimer's disease. To aid in understanding and provide visual context, MR images from each of the four categories (ND, MoD, MD, and VMD) are included in the study.

B. Evaluation Parameters

Table 1: Evaluation parameters

TP (True Positive)	"Number of individuals with Alzheimer's disease correctly classified"
TN (True Negative)	"Number of healthy individuals correctly classified as not having Alzheimer's disease"
FP (False Positive)	"Number of healthy individuals incorrectly classified as having Alzheimer's disease"
FN (False Negative)	"Number of individuals with Alzheimer's disease incorrectly classified as healthy"

$$Accuracy = \frac{TP + TN}{TP + TN + FP + FN} \quad (45)$$

$$Precision = \frac{TP}{TP + FP} \quad (46)$$

$$Sensitivity = \frac{TP}{TP + FN} \quad (47)$$

$$Specificity = \frac{TN}{TN + FN} \quad (48)$$

$$Error\ Rate = \frac{FP + FN}{TP + TN + FP + FN} \quad (49)$$

$$False\ Positive\ Rate(FPR) = \frac{FP}{FP + TN} \quad (50)$$

$$F - Score = \frac{2TP}{2TP + FP + FN} \quad (51)$$

$$Matthews\ Correlation\ Coefficient\ (MCC) = \frac{(TP \times TN) - (FP \times FN)}{\sqrt{(TP+FN)(TP+FP)(TN+FN)(TN+FP)}} \quad (52)$$

$$Kappa\ Statistics = \frac{2(TP \times TN - FN \times FP)}{(TP+FP) \times (FP+TN) + (TN+FN) \times (FN+TN)} \quad (53)$$

C. Results

The confusion matrix plots for the Alzheimer's Disease detection using different classifiers—KNN, SVM, Neural Network, and ESO-Optimized Neural Network (Figure 4-Figure 7)—provide detailed insights into the classification performance across four stages of dementia: Non Demented, Moderate Demented, Mild Demented, and Very Mild Demented. Each plot displays the number of correctly classified cases (true positives) along the diagonal and misclassifications (false positives and false negatives) in the off-diagonal cells.

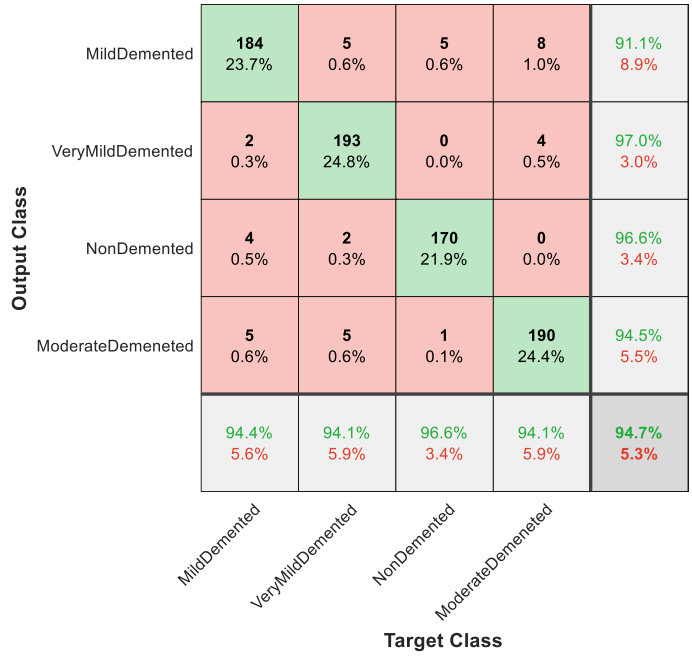

Figure 4: Confusion Matrix Plot for Proposed Alzheimer's Disease Detection using KNN Classifier

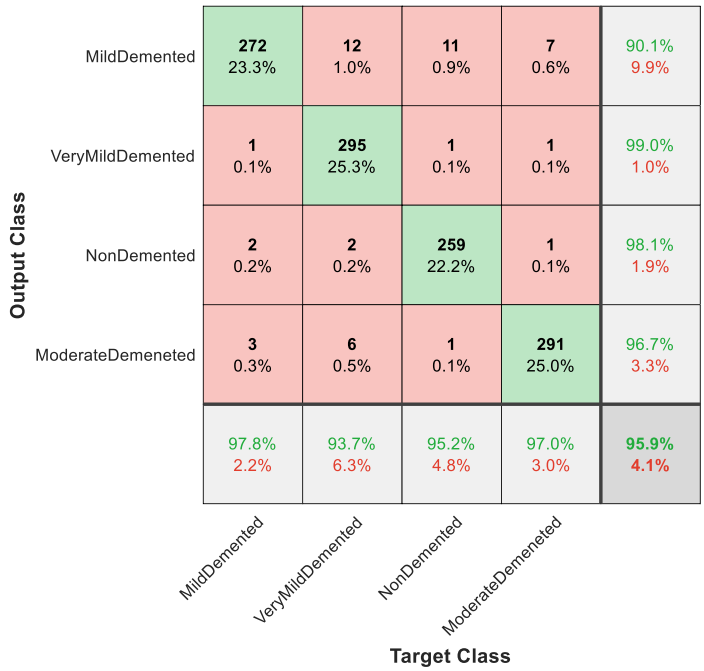

Figure 5: Confusion Matrix Plot for Proposed Alzheimer's Disease Detection using SVM Classifier

The KNN matrix highlights its ability to distinguish between stages with moderate accuracy, while the SVM matrix reflects its robust performance but with some misclassification. The Neural Network matrix shows high effectiveness in identifying dementia stages, and the ESO-Optimized Neural Network matrix, with its enhanced classification accuracy and minimized misclassifications, demonstrates superior performance achieved through optimization.

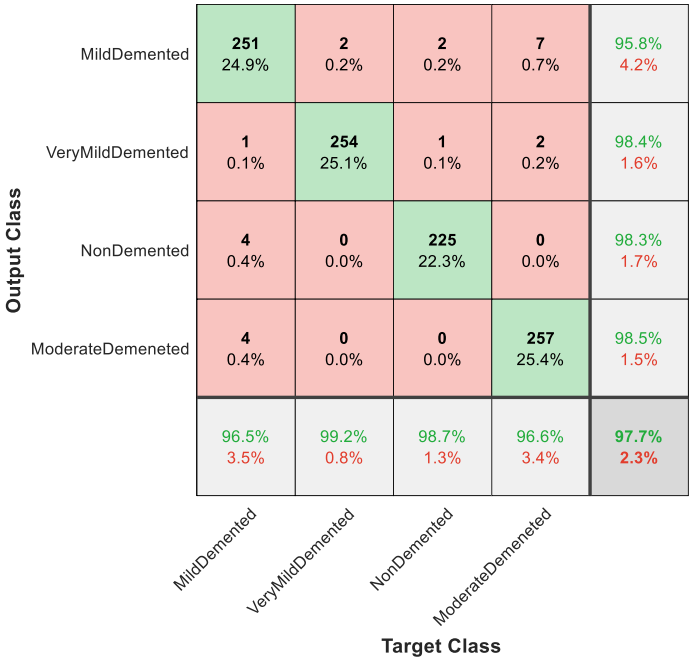

Figure 6: Confusion Matrix Plot for Proposed Alzheimer's Disease Detection using Neural Network Classifier

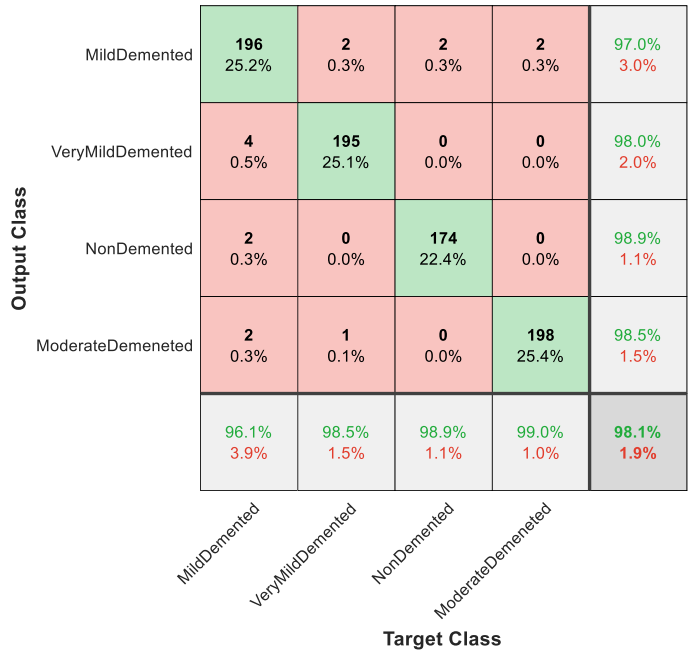

Figure 7: Confusion Matrix Plot for Proposed Alzheimer's Disease Detection using ESO-Optimized Neural Network Classifier

Figure 8 displays the distribution of training data across different classes, illustrating how samples are allocated for model training. Figure 9 provides a breakdown of the number of images available for each class, highlighting the dataset's composition. Figure 10 presents a graphical comparison of loss versus epochs, showcasing the model's learning progress and convergence behavior during training and validation. Similarly, Figure 11 compares accuracy versus epochs, revealing how the model's performance improves over time for both training and validation phases.

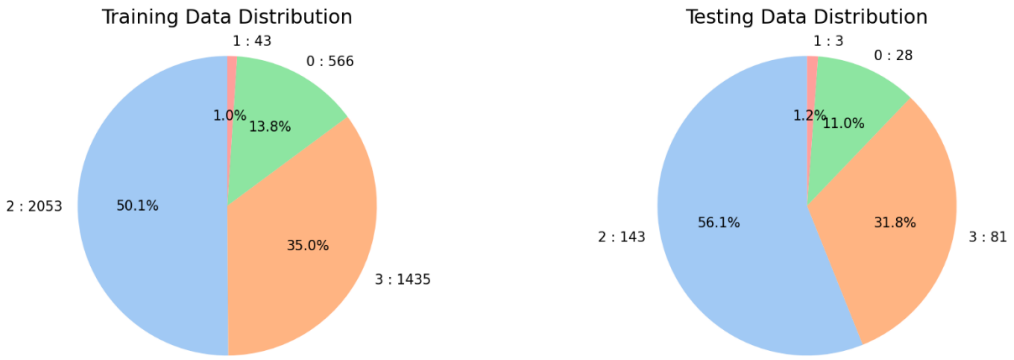

Figure 8: Training data distribution graphs for the proposed work

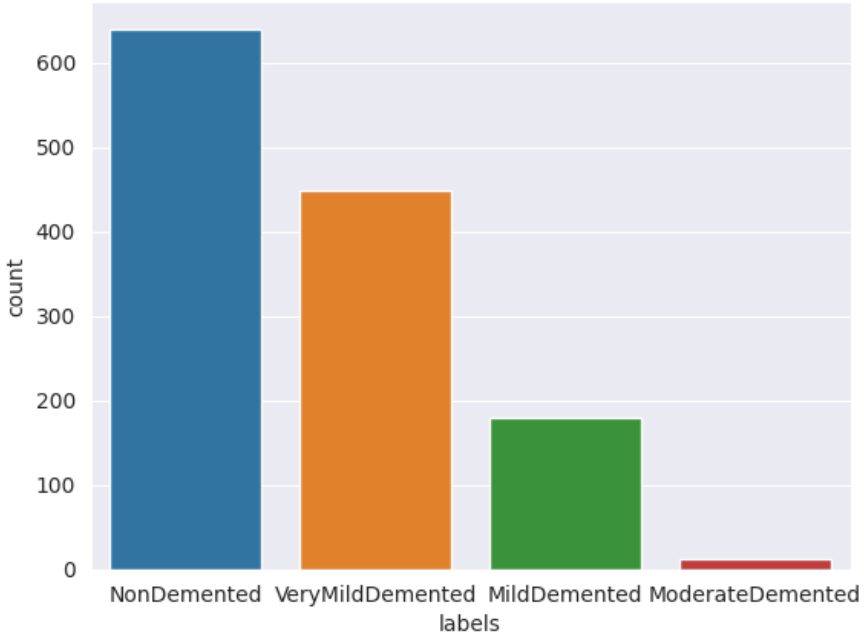

Figure 9: Number of images of each class for all data

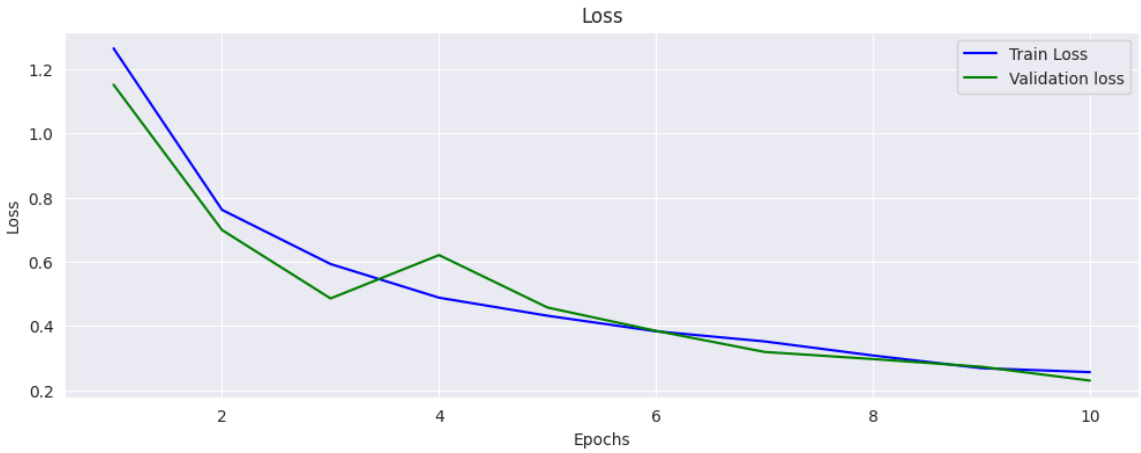

Figure 10: Graphical comparison of loss vs. epochs for training and validation

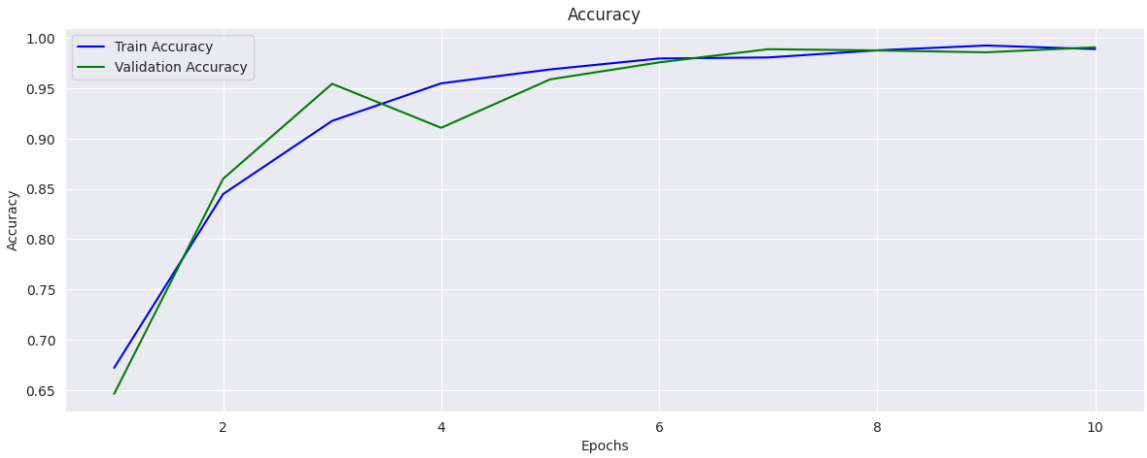

Figure 11: Graphical comparison of accuracy vs. epochs for training and validation

Table 2: Results analysis for various classification techniques

Parameters	KNN	SVM	NN	ESO-Optimized NN
Accuracy	94.73%	95.88%	97.72%	98.07%
Error Rate	5.27%	4.12%	2.28%	1.93%
Sensitivity	94.79%	95.93%	97.76%	98.11%
Specificity	98.24%	98.64%	99.24%	99.35%
Precision	94.80%	95.96%	97.74%	98.10%
False Positive Rate	1.76%	1.36%	0.76%	0.65%
F1-Score	94.78%	95.88%	97.75%	98.10%
MCC	93.03%	94.56%	96.99%	97.46%
Kappa	85.95%	89.01%	93.93%	94.86%

Table 2 provides a comprehensive analysis of various classification techniques including KNN, SVM, Neural Network (NN), and ESO-Optimized NN by comparing several performance metrics. For the KNN, SVM, and NN classifiers, the accuracy is recorded as 94.73%, 95.88%, and 97.72%, respectively, showing a progressive improvement in classification accuracy as the techniques become more sophisticated. In contrast, the ESO-Optimized NN classifier demonstrates superior performance across all parameters with an accuracy of 98.07%, the lowest error rate of 1.93%, sensitivity of 98.11%, specificity of 99.35%, precision of 98.10%, an F1-Score of 98.10%, an MCC of 97.46%, and a Kappa statistic of 94.86%. These values underscore the ESO-Optimized NN's enhanced ability to accurately classify Alzheimer's disease stages, exhibiting the highest precision, recall, and overall performance among the classifiers evaluated.

Table 3: Performance comparison of proposed work with previous research works

Method	Dataset Source	No. of Images	Techniques Used	Accuracy
[20]	ADNI	177	DenseNet-201	84.38%
			ResNet50	81.25%
[21]	ADNI	1167	SVM with D.L.	75%
[22]	ADNI	3127	2D-CNN with D.L.	82.57%
[23]	OASIS	416	Cross-Modal Transfer Learning	83.57%

[24]	OASIS	416	DTCWT and PCA with FNN	90.06%
Proposed Methodology	**OASIS-3**	**6400**	**KNN**	**94.73%**
			SVM	**95.88%**
			NN	**97.72%**
			ESO-Optimized NN	**98.07%**

Table 3 provides a comparative analysis of the performance of various methods in Alzheimer's disease classification based on their accuracy rates and datasets used. The table lists multiple approaches, starting with methods from the ADNI dataset: the authors of [20] employed DenseNet-201 and ResNet50, achieving accuracies of 84.38% and 81.25%, respectively; the authors of [21] utilized an SVM with deep learning techniques, which resulted in a 75% accuracy; and the authors of [22] applied a 2D-CNN with deep learning, reaching an accuracy of 82.57%. The OASIS dataset was used in the authors of [23], which employed Cross-Modal Transfer Learning and achieved an accuracy of 83.57%, while the authors of [24] used DTCWT and PCA with a feed-forward neural network (FNN), attaining the highest accuracy among previous works at 90.06%. In comparison, the proposed methodology, tested on the OASIS-3 dataset, outperforms all prior methods with a substantial number of 6,400 images. It employs several techniques, including KNN with an accuracy of 94.73%, SVM achieving 95.88%, NN at 97.72%, and an ESO-Optimized NN that leads with the highest accuracy of 98.07%.

6. CONCLUSION

The proposed framework demonstrates a robust approach for Alzheimer's disease detection through the integration of advanced image processing and machine learning techniques. By leveraging CLAHE for contrast enhancement and employing a suite of feature extraction methods—DWT-LBP for texture, HOG for structural features, and SURF-BoW for key point detection—the system effectively captures diverse image characteristics. The combined feature vector, optimized through NCA, enhances the discriminative power of the classification models. Notably, this research surpasses the accuracy levels reported in previous studies, achieving the highest accuracy of 98.07% with the ESO-optimized Neural Networks (ESO-NN) approach. The application of SVM, KNN, and ESO-NN offers a comprehensive evaluation of the detection system's performance, with significant improvements in classification accuracy and reliability. This multi-layered approach, combining image preprocessing, feature extraction, and advanced classification, represents a significant advancement in diagnostic capabilities for Alzheimer’s disease, paving the way for more accurate and early detection. Future research could explore the integration of additional modalities, such as genetic or physiological data, to further enhance detection accuracy and develop personalized diagnostic tools. Additionally, extending the framework to real-world clinical settings and large-scale datasets could validate and refine its effectiveness in diverse populations.

REFERENCES

[1] Dubois, Bruno, Gaetane Picard, and Marie Sarazin. “Early detection of Alzheimer's disease: new diagnostic criteria.” Dialogues in clinical neuroscience (2022).

[2] Basheera, Shaik, and M. Satya Sai Ram. “Convolution neural network–based Alzheimer's disease classification using hybrid enhanced independent component analysis based segmented gray matter of T2 weighted magnetic resonance imaging with clinical valuation.” Alzheimer's & Dementia: Translational Research & Clinical Interventions 5 (2022): 974-986.

[3] Janghel, R. R., and Y. K. Rathore. “Deep convolution neural network-based system for early diagnosis of Alzheimer's disease.” Irbm 42, no. 4 (2024): 258-267.

[4] Marwa, EL-Geneedy, Hossam El-Din Moustafa, Fahmi Khalifa, Hatem Khater, and Eman AbdElhalim. “An MRI-based deep learning approach for accurate detection of Alzheimer’s disease.” Alexandria Engineering Journal 63 (2023): 211-221.

[5] Zhang, Fan, Zhenzhen Li, Boyan Zhang, Haishun Du, Binjie Wang, and Xinhong Zhang. “Multi-modal deep learning model for auxiliary diagnosis of Alzheimer’s disease.” Neurocomputing 361 (2022): 185-195.

[6] Bhatkoti, Pushkar, and Manoranjan Paul. “Early diagnosis of Alzheimer's disease: A multi-class deep learning framework with modified k-sparse autoencoder classification.” In 2023 international conference on image and vision computing New Zealand (IVCNZ), pp. 1-5. IEEE, 2023.

[7] Feng, Chiyu, Ahmed Elazab, Peng Yang, Tianfu Wang, Feng Zhou, Huoyou Hu, Xiaohua Xiao, and Baiying Lei. “Deep learning framework for Alzheimer’s disease diagnosis via 3D-CNN and FSBi-LSTM.” IEEE Access 7 (2022): 63605-63618.

[8] Islam, J., and Y. Zhang. "Brain MRI analysis for Alzheimer's disease diagnosis using an ensemble system of deep convolutional neural networks. Brain Inf 2023; 5: 2. doi: 10.1186/s40708-018-0080-3 2.

[9] Liu, Manhua, Fan Li, Hao Yan, Kundong Wang, Yixin Ma, Li Shen, Mingqing Xu, and Alzheimer's Disease Neuroimaging Initiative. "A multi-model deep convolutional neural network for automatic hippocampus segmentation and classification in Alzheimer's disease." Neuroimage 208 (2020): 116459.

[10] Neffati, Syrine, Khaoula Ben Abdellafou, Ines Jaffel, Okba Taouali, and Kais Bouzrara. "An improved machine learning technique based on downsized KPCA for Alzheimer's disease classification." International Journal of Imaging Systems and Technology 29, no. 2 (2022): 121-131.

[11] Sarraf, Saman, and Ghassem Tofighi. "Classification of alzheimer's disease using fmri data and deep learning convolutional neural networks." arXiv preprint arXiv:1603.08631 (2022).

[12] Cui, Zhenyu, Zhiao Gao, Jiaxu Leng, Tianlin Zhang, Pei Quan, and Wei Zhao. "Alzheimer's disease diagnosis using enhanced inception network based on brain magnetic resonance image." In 2022 IEEE international conference on bioinformatics and biomedicine (BIBM), pp. 2324-2330. IEEE, 2022.

[13] Jabason, Emimal, M. Omair Ahmad, and M. N. S. Swamy. "Classification of Alzheimer's Disease from MRI Data Using a Lightweight Deep Convolutional Model." In 2022 IEEE International Symposium on Circuits and Systems (ISCAS), pp. 1279-1283. IEEE, 2022.

[14] Shahbaz, Muhammad, Shahzad Ali, Aziz Guergachi, Aneeta Niazi, and Amina Umer. "Classification of Alzheimer's Disease using Machine Learning Techniques." In Data, pp. 296-303. 2024.

[15] Tuan, Tran Anh, The Bao Pham, Jin Young Kim, and Joao Manuel RS Tavares. "Alzheimer's diagnosis using deep learning in segmenting and classifying 3D brain MR images." International Journal of Neuroscience 132, no. 7 (2022): 689-698.

[16] Khatri, Uttam, and Goo-Rak Kwon. "Alzheimer's disease diagnosis and biomarker analysis using resting-state functional MRI functional brain network with multi-measures features and hippocampal subfield and amygdala volume of structural MRI." Frontiers in aging neuroscience 14 (2022): 818871.

[17] Tu, Yue, Shukuan Lin, Jianzhong Qiao, Yilin Zhuang, and Peng Zhang. "Alzheimer's disease diagnosis via multimodal feature fusion." Computers in Biology and Medicine 148 (2022): 105901.

[18] Kim, Mansu, Jaesik Kim, Jeffrey Qu, Heng Huang, Qi Long, Kyung-Ah Sohn, Dokyoon Kim, and Li Shen. "Interpretable temporal graph neural network for prognostic prediction of Alzheimer's disease using longitudinal neuroimaging data." In 2024 IEEE International Conference on Bioinformatics and Biomedicine (BIBM), pp. 1381-1384. IEEE, 2024.

[19] Venugopalan, Janani, Li Tong, Hamid Reza Hassanzadeh, and May D. Wang. "Multimodal deep learning models for early detection of Alzheimer's disease stage." Scientific reports 11, no. 1 (2024): 3254.

[20] Ebrahimi-Ghahnavieh, Amir, Suhuai Luo, and Raymond Chiong. "Transfer learning for Alzheimer's disease detection on MRI images." In 2022 IEEE International Conference on Industry 4.0, Artificial Intelligence, and Communications Technology (IAICT), pp. 133-138. IEEE, 2022.

[21] Rallabandi, VP Subramanyam, Ketki Tulpule, Mahanandeeshwar Gattu, and Alzheimer's Disease Neuroimaging Initiative. "Automatic classification of cognitively normal, mild cognitive impairment and Alzheimer's disease using structural MRI analysis." Informatics in Medicine Unlocked 18 (2023): 100305.

[22] Feng, Wei, Nicholas Van Halm-Lutterodt, Hao Tang, Andrew Mecum, Mohamed Kamal Mesregah, Yuan Ma, Haibin Li et al. "Automated MRI-based deep learning model for detection of Alzheimer's disease process." International Journal of Neural Systems 30, no. 06 (2023): 2050032.

[23] Aderghal, Karim, Alexander Khvostikov, Andrei Krylov, Jenny Benois-Pineau, Karim Afdel, and Gwenaelle Catheline. "Classification of Alzheimer disease on imaging modalities with deep CNNs using cross-modal transfer learning." In 2023 IEEE 31st international symposium on computer-based medical systems (CBMS), pp. 345-350. IEEE, 2023.

[24] Jha, Debesh, Ji-In Kim, and Goo-Rak Kwon. "Diagnosis of Alzheimer's disease using dual-tree complex wavelet transform, PCA, and feed-forward neural network." Journal of healthcare engineering (2022).

[25] LaMontagne, Pamela J., Tammie LS Benzinger, John C. Morris, Sarah Keefe, Russ Hornbeck, Chengjie Xiong, Elizabeth Grant et al. "OASIS-3: longitudinal neuroimaging, clinical, and cognitive dataset for normal aging and Alzheimer disease." MedRxiv (2019): 2022-12.